**Supplementary Materials for the Article**

# "Wavelet-transformed temporal cerebral blood flow signals during attempted inhibition of cue-induced cocaine craving distinguish prognostic phenotypes"

Shing Chun Benny Lam[1], Ze Wang[1], Yin Li[1], Teresa Franklin[1], Charles O'Brien[1], Jeremy Magland[2], Anna Rose Childress[1]

[1]Department of Psychiatry, University of Pennsylvania, Philadelphia, PA 19104, USA
[2]Department of Radiology, University of Pennsylvania, Philadelphia, PA 19104, USA

Submitted to Drug and Alcohol Dependence.

For more information, contact Anna Rose Childress, Department of Psychiatry, University of Pennsylvania Philadelphia, PA 19104, USA Phone: +1 215 222 3200 childres@mail.med.upenn.edu

## 1. Methods

### Time-frequency analysis and wavelet transform coherence

Wavelet transform (Mallat, 1989) is a versatile tool to characterize the signal at different time-frequency resolution by representing the original signal (the mean rCBF signal $X(n)$ here) with a series of scaled and time translated versions of a mother wavelet function $\psi_0$ via convolution:

$$W_X(n,s) = \sqrt{\frac{\Delta t}{s}} \sum_{n'=1}^{N} X(n) \psi_0^* \left[ (n'-n) \left( \frac{\Delta t}{s} \right) \right], \quad (1)$$

where $n$ is the time index, $N$ is the total number of time points, $\Delta t$ is the sampling step size and $f$ is the wavelet scale analogous to frequency. Here, we chose the complex Morlet wavelet $\psi_0(\xi) = \pi^{-1/4} e^{i\omega_0 \xi} e^{-\xi^2/2}$ as our mother wavelet with $\omega_0 = 6$ as it has been vigorously validated theoretically and experimentally for spectral analysis of biological and time-varying signals (Chang and Glover, 2010; Lachaux et al., 2002). $W_X(n,s)$ is a complex quantity in which its modulus $|W_X(n,s)|$ and phase angle $\tan^{-1}\left( \mathrm{Im}\{W_X(n,s)\} / \mathrm{Re}\{W_X(n,s)\} \right)$ represent the local power and phase of $X$ as a function of time and frequency respectively. Cross wavelet transform between two signals $X$ and $Y$ can be calculated as:

$$W_{XY}(n,s) = W_X(n,s) W_Y^*(n,s), \quad (2)$$

where $W_Y^*$ is the complex conjugate of $W_X$. The wavelet transform coherence (WTC), which is analogous to time and frequency localized correlation coefficient, is defined as:

$$R^2(n,s) = \frac{\left| \left\langle s^{-1} W_{XY}(n,s) \right\rangle \right|^2}{\left| \left\langle s^{-1} W_X(n,s) \right\rangle \right|^2 \left| \left\langle s^{-1} W_Y(n,s) \right\rangle \right|^2}, \quad (3)$$

and the wavelet-coherency phase difference, which is also localized in time and frequency, is given by:

$$\phi(n,s) = \tan^{-1} \left( \frac{\mathrm{Im}\left\{ \left\langle s^{-1} W_{XY}(n,s) \right\rangle \right\}}{\mathrm{Re}\left\{ \left\langle s^{-1} W_{XY}(n,s) \right\rangle \right\}} \right), \quad (4)$$

where $\langle \cdot \rangle$ is the smoothing operator in both time and frequency. The filter for temporal and scale smoothing are Gaussian and boxcar function respectively (Torrence and Webster, 1999). The range of $R^2$ is between 0 and 1 while the range of $\phi$ is between $-\pi$ and $\pi$.

Due to the low frequency nature of the rCBF signals, WTC results are presented in terms of period ($T$ = 1/frequency) to avoid long decimal numbers. The coherency phase difference between $X$ and $Y$ at each period and time is presented with an overlaid phasor diagram in which the arrow pointing horizontally right and left indicating the two signals are completely in phase ($\phi = 0$) and out of phase ($\phi = \pi$), respectively. Implementation of WTC was based on the Matlab wavelet coherence package from (Grinsted et al., 2004).

**Statistical testing of WTC temporal and magnitude variability with bootstrapping**

The statistical significance of the temporal pattern variation and magnitude of the WTC between *X* and *Y* was tested using a Monte Carlo method based on time-series bootstrapping using the detailed procedures described in Chang and Glover (Chang and Glover, 2010). Briefly, the rCBF time series of individual patients were fitted into a stationary vector autoregressive (VAR) model. The data fitting residuals of *X* and *Y* were randomly resampled 1000 times and were subsequently fed into the same VAR model to generate 1000 new time series for both *X* and *Y* (*X'* and *Y'*). WTC was calculated for each pair of *X'* and *Y'.* Variance was then calculated for each *s*, after which a null distribution of variance was generated for each *s* across all simulated signals. If the variance from real data fell outside the confidence interval (95%) of the null distribution, that *s* was considered statistically non-significant. Similarly, to test the magnitude of $R^2$, magnitudes of WTC were calculated from 300 simulated time signals generated using the same VAR model parameters. The $R^2$ at *s* was considered to be non-significant if the variance from real data fell outside the confidence interval of the null distribution from the simulation. As the VAR model is independent of the sampling rate (i.e. TR), this bootstrapping test actually guarantees the statistical significance of WTC results for each individual regardless of his TR. The periods and times that passed the test were bounded with thick black contours (Figure 1).

**References:**


Chang, C., Glover, G.H., 2010. Time-frequency dynamics of resting-state brain connectivity measured with fMRI. Neuroimage 50, 81-98.

Grinsted, A., Moore, J.C., Jevrejeva, S., 2004. Application of the cross wavelet transform and wavelet coherence to geophysical time series. Nonlinear Processes in Geophysics 11, 561-566.

Lachaux, J.P., Lutz, A., Rudrauf, D., Cosmelli, D., Le Van Quyen, M., Martinerie, J., Varela, F., 2002. Estimating the time-course of coherence between single-trial brain signals: an introduction to wavelet coherence. Neurophysiol Clin 32, 157-174.

Mallat, S.G., 1989. A theory for multiresolution signal decomposition: the wavelet represetation. IEEE transactions on pattern analysis and machine intelligence 11, 674-693.

Torrence, C., Webster, P., 1999. Interdecadal changes in the ENSO-Monsoon system. Journal of climate 12, 2679-2690.

**Table S1. fMRI sequences and parameters**

| Subject | Sequence | TR(s) | TE(ms) | Labeling time (s) | Post labeling delay (s) | Thickness (mm) | Inter-slice spacing (mm) | Number of slices |
|---|---|---|---|---|---|---|---|---|
| N1 | PASL | 2 | 17 | 2 | 0.8 | 6 | 1.5 | 12 |
| N2 | PASL | 2 | 17 | 2 | 0.8 | 6 | 1.5 | 12 |
| N3 | PASL | 2 | 17 | 2 | 0.8 | 6 | 1.5 | 12 |
| N4 | PASL | 2 | 17 | 2 | 0.8 | 6 | 1.5 | 12 |
| N5 | PASL | 2 | 17 | 2 | 0.8 | 6 | 1.5 | 12 |
| N6 | CASL | 3.75 | 17 | 1.6 | 1 | 8 | 2 | 14 |
| N7 | CASL | 3.75 | 17 | 1.6 | 1 | 8 | 2 | 14 |
| N8 | CASL | 3.75 | 17 | 1.6 | 1 | 8 | 2 | 14 |
| P1 | PASL | 2 | 17 | 2 | 0.8 | 6 | 1.5 | 12 |
| P2 | PASL | 2 | 17 | 2 | 0.8 | 6 | 1.5 | 12 |
| P3 | PASL | 2 | 17 | 2 | 0.8 | 6 | 1.5 | 12 |
| P4 | PASL | 2 | 17 | 2 | 0.8 | 6 | 1.5 | 12 |
| P5 | PASL | 2 | 17 | 2 | 0.8 | 6 | 1.5 | 12 |
| P6 | CASL | 3 | 17 | 1.6 | 0.7 | 8 | 2 | 14 |
| P7 | CASL | 3 | 17 | 1.6 | 0.7 | 8 | 2 | 14 |
| P8 | CASL | 3 | 17 | 1.6 | 0.7 | 8 | 2 | 14 |
| P9 | CASL | 3.75 | 17 | 1.6 | 1 | 8 | 2 | 14 |
| P10 | CASL | 3.75 | 17 | 1.6 | 1 | 8 | 2 | 14 |
| P11 | CASL | 3.75 | 17 | 1.6 | 1 | 8 | 2 | 14 |

Notes:
1. All scans have in-plane resolution of 3.4 $mm^2$ and matrix size of 64×64.
2. Subjects N1 – N8: Cocaine-negative entry urine (CocNeg); P1 – P11: Cocaine-positive entry urine (CocPos).
3. PASL: Pulse Arterial Spin Labeling; CASL: Continuous Arterial Spin Labeling.
4. CocNeg and CocPos subjects are distributed across both PASL and CASL.
5. TR: Repetition time; TE: Echo time.

## 2. Supporting results

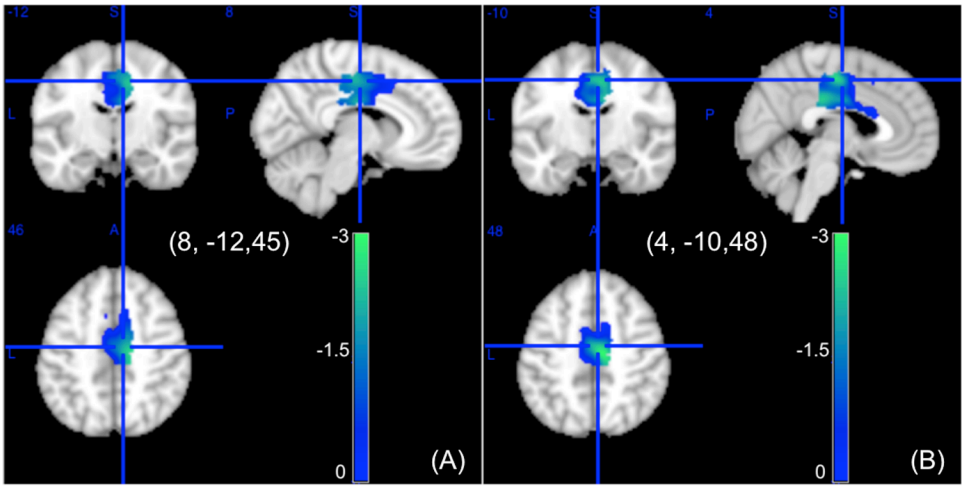


**Figure S1.** Group-level threshold t-maps for negative correlations with (A) left and (B) right amygdala with the location having the maximum t-value indicated. The coordinates are in MNI space. A sphere of 3mm around the indicated voxel was taken as the ROI to for WTC analysis.

To investigate the distribution of phase related to the amount of time in the task, the phase difference $\phi$ between amygdala and dCC rCBF at the times and periods having significant coherence were binned into one of the four classes of phase difference: 0±π/4, π/2±π/4, π±π/4 or 3π/4±π/4. Thus, the accumulated time (i.e., total duration) at each period is the count of the binned $\phi$ in each of the four classes. Figure S2 shows the accumulated duration of coherence averaged across all subjects in each group. In the CocNeg group, $\phi$ = π was the most prevalent in both sides of the amygdalae across all periods (Figure S2A and B) suggesting that the amygdala and dCC rCBF were mainly antiphase in the CocNeg group. On the other hand, $\phi$ = 0 was very rare which suggests that the rCBF signals between amygdala and dCC in the CocNeg group were rarely in-phase. Phase differences of π had slightly longer duration only in the initial periods (left: $T$ < 38s; right: $T$ < 22s). The other three $\phi$ classes occupied the rest of the spectrum (Figure 2C and D). Comparing the $\phi$ values between the two groups, there were significant differences in $\phi$ = 0 and π in both sides (both $p < 2\times10^{-6}$, ANOVA). This demonstrated that the rCBF signals between amygdala and dCC in CocNeg and CocPos group were primarily antiphase and in-phase, respectively. There was no significant difference in duration among the periods within the groups (all $p > 0.46$, ANOVA).

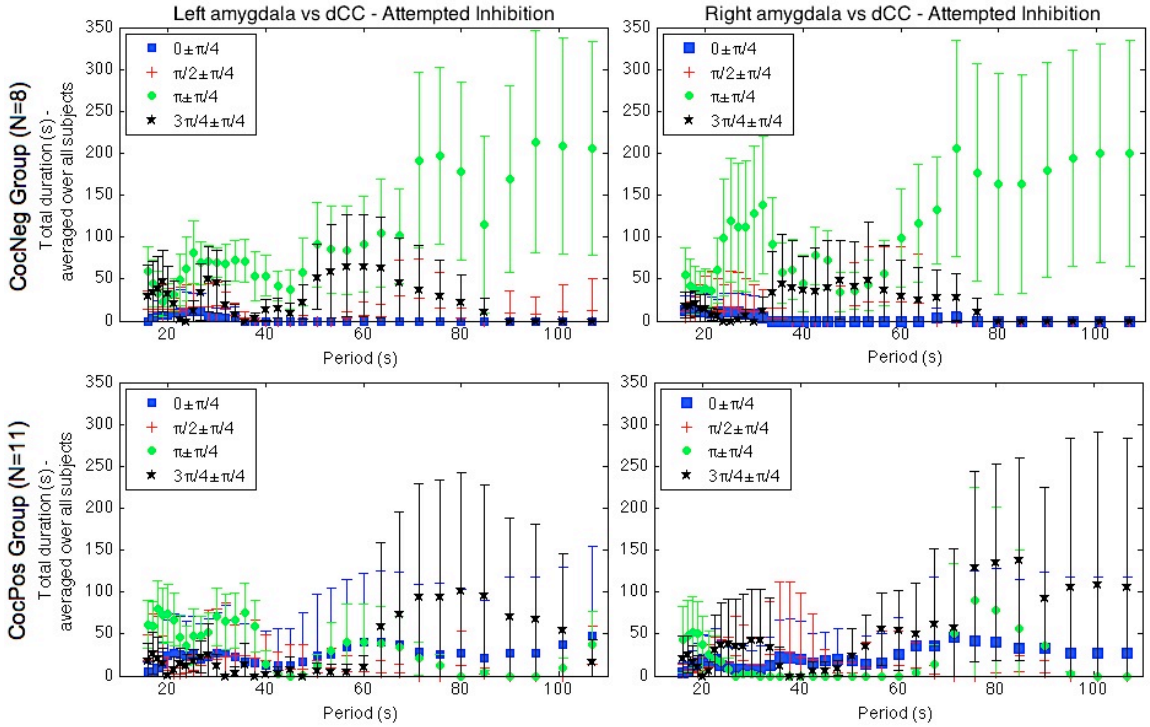


**Figure S2.** Durations of $\pi$ phase difference (antiphase) between the amygdala and dCC ROI were significantly longer in the CocNeg group (top row) than in the CocPos group (bottom row) for both left (left column) and right (right column) over all periods. Each longitudinal line represents the mean total duration of coherence of the corresponding phase across subjects in each group, and error bar represents standard error.

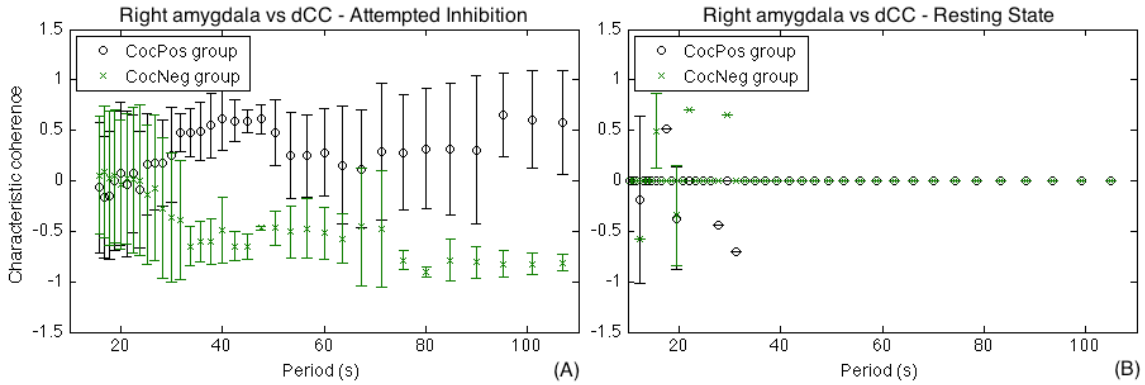


**Figure S3.** The CocNeg group demonstrated more negative characteristic coherence *K* than the CocPos group between right amygdala and dCC ROI (A). In contrast, this relationship is absent during the resting state (B). Each longitudinal point (circle/cross) represents the mean *K* across subjects in the 2 groups, and error bar represents standard error.

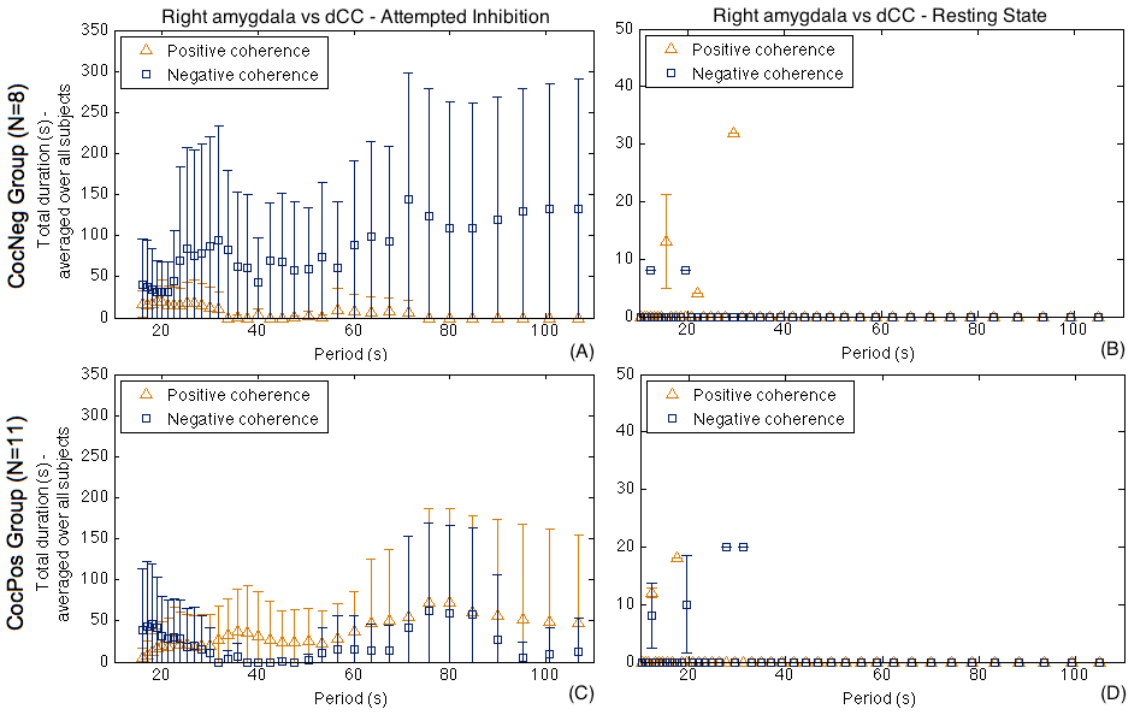


**Figure S4.** The CocNeg group (top row) had longer duration of negative coherence (blue squares) between right amygdala and corresponding dCC ROI as compared to the CocPos group (A and C). This relationship was absent during the resting state (B and D). Each longitudinal point (triangle/square) represents the mean total duration of the corresponding characteristic coherence *K* across the subjects in the 2 groups, and error bar represents standard error.

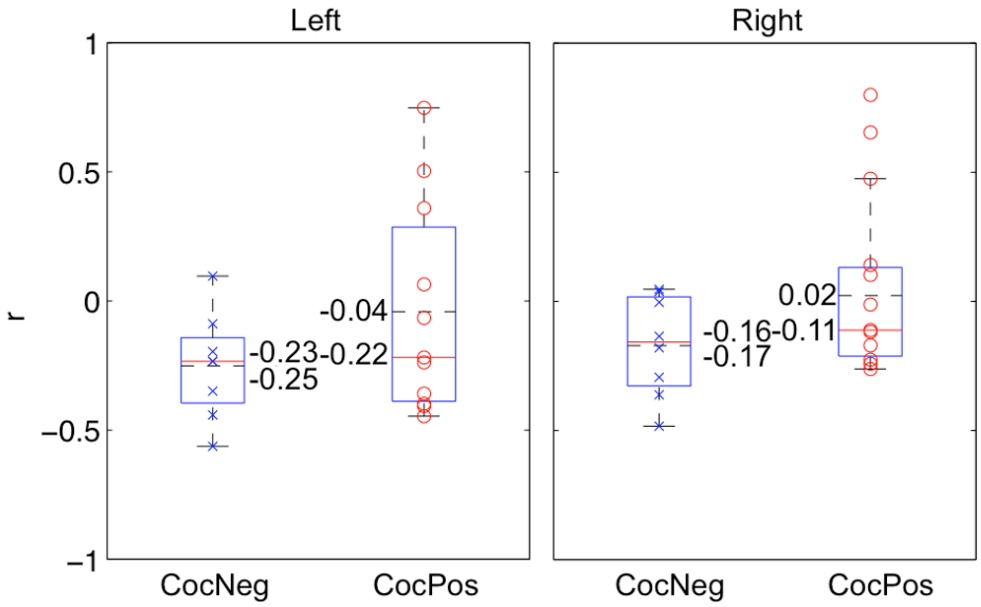


**Figure S5.** CocNeg group had a more negative correlation than CocPos group in the time series rCBF signals between (A) left and (B) right amygdala and dCC ROI. The horizontal black and red line inside the blue box indicates the group mean and median respectively. The upper and lower edges of the blue box are the 75$^{th}$ and 25$^{th}$ percentiles.